Self-Calibration of Fused Camera Images

Karsten Jacobsen [1]

[1] Institute of Photogrammetry and GeoInformation, Leibniz Universität Hannover, Germany - jacobsen@ipi.uni-hannover.de
Commission I

Keywords: self-calibration, fused camera images, bundle adjustment, image geometry

ABSTRACT:

The standard sensor for large-format digital cameras is currently the Sony CMOS chip with approximately 14200 x 10600 pixels of 3.76 µm. Sony CMOS chips with ~ 19299 x 12800 pixels and a pixel size of 2.81 µm will be available in near future. The very large sensors used in the DMC-3 are no longer manufactured. To achieve larger imaging systems, camera systems with multiple sub-cameras are being used instead of single cameras. The images of the sub-cameras must be fused into homogenous images. The dominant method for the image fusion is the geometric fusion of the sub-images to lower resolution overview images. To achieve this, the images are geometrical enhanced by the calibrating the sub-cameras. Theoretically, the fused, geometrical enhanced images should be free of systematic image errors. However, this must not be the case, even with thermal control of the sub-cameras, satisfying thermal camera control of the entire camera system is not possible. The standard additional parameters cannot be used for image fusion problems that do not meet the calibration of individual cameras. Therefore, a specific set of additional parameters is required for each type of fused images. It turns out that full geometric accuracy can only be achieved with such special set of additional parameters, but it is possible to reach the accuracy as for the single cameras.

1. Introduction

Due to the limited size of available CMOS sensors, camera systems are becoming popular. The fused images of such camera systems can be affected by systematic image errors of the camera system. Therefore, a specific set of additional parameters is required for each camera system type.

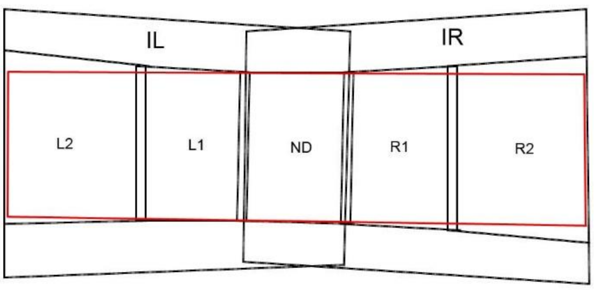

Figure 1: Configuration of PhaseOne PAS Pana camera system, red = used fused image part
IL, IR = infrared cameras +/-14° nadir angle
RGB-cameras at nadir, +/-13°and at +/-27° nadir angles

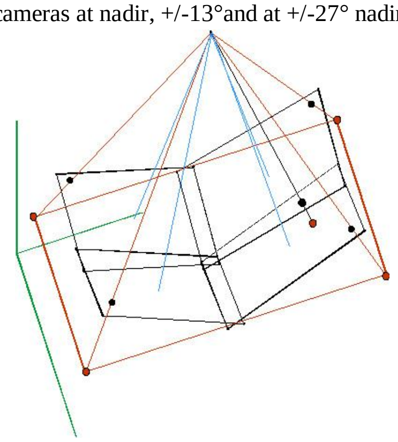

Figure 2: Configuration of the DMC-1 camera system

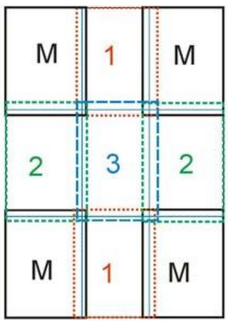

Figure 3: Configuration of UltraCam Eagle sub-images

Figures 1 up to 3 shows some of these camera systems. Before the sub-images are fused, their geometry is improved by the camera calibration of the single cameras. Theoretically, therefore, the fused images should be free of systematic image errors, but this is not the case on the highest accuracy level.

The PhaseOne PAS Pana has fife red, green and blue (RGB) cameras plus 2 near infrared (NIR) cameras with a shorter focal length, that cover the whole imaged area (Figure 1). The NIR cameras image the area with a larger overlap, enabling satisfactory fusion of the NIR images. The overlap of the RGB cameras is limited and cannot guarantee a satisfying stitching of the RGB images. Therefore, the fused NIR images are used as reference for the fusion of the RGB images (Jacobsen et al. 2025).

The DMC-1 has 4 slightly inclined sub-cameras (Figure 2), arranded in a square pattern. This has the advantage that the geometry of each sub-image combination can be controled by a bundle adjustment with fixed projection centers (Doerstel et al. 2002). However, also with this very precise solution, the highest accuracy can only be achieved with special additional parameters for the image configuration.

The Vexcel UltraCam Eagle camera configuration uses four subcameras with in total nine sensors for the panchromatic bands in a planar configuration (Leberl et al. 2002). The master cone (M im Figure 3) has four sensors, two cones have two sensors each (1 and 2 in Figure 3), and one cone has one sensor in the center. The sub-images are fused using the subcamera for the green channel which covers the entire area at a linear 3 times smaller scale (Gruber and Ladstaedter 2006). Even with this camera configuration, special additional parameters can improve the geometry of the fused images.

2. Additional parameters for the fused images

The required systematic image errors of single-camera images and fused camera images can be identified by analysing the remaining systematic image errors of a bundle block adjustment. Remaining systematic image errors after block adjustment with or without additional parameters can be analysed using the residuals at the image coordinates after the bundle adjustment. By superimposing all image residuals in one image plane, averaging can be performed in a grid of small image sub areas (Jacobsen et al. 2010). Based on the remaining systematic image errors determined in this way, the set of additional parameters can be extended to cover these effects. This method also offers the advantage of avoiding strong correlations between the parameters.

Various sets of additional parameters are used. Self-calibration with additional parameters in bundle block adjustments started with the publication of (Brown 1971). Based on the theoretical investigation of decentred lens systems (Conradi 1919), he published the first set of additional parameters, named Brown-Conradi or also Australis (2) and (3). This set has a physical basis. Schut used another method. He generated a set of 7 parameters using third order polynomials of image coordinate x and y (Schut 1974). This was extended by Ebner to eliminate the systematic image errors at a regular grid of 3 x 3 image positions (Ebner 1976) (Grün 1978). Grün extend this to 44 parameters, which corresponds to a regular grid of 5 x 5 image positions (Grün and Beyer 2001).

The Ebner and Grün polynomial parameters have the disadvantage that the currently dominant radial symmetric parameters cannot be expressed directly, but can only can be approximated by a number of other parameters. The 44 Grün parameters must be reduced to the required ones, especially for smaller blocks. The Brown-Conradi parameters have the disadvantage of a strong correlation between the parameters to the focal length. The affinity and angular affinity parameters (3) only influence to the x-image coordinate, causing a correlation to the focal length. In the BLUH program (Jacobsen 1980), these correlations for the affinity and angular affinity are avoided by an equal influence to the x- and y-image coordinate (4, parameters 1 and 2). The strong correlation of the radial symmetric parameters to the focal length in BLUH is eliminated by a zero crossing of the radial symmetric distortion and an internal scaling of the image coordinates as function of the image format (4, parameter 9). The basic set of the parameters for the Hannover program BLUH is a combination of the physically justified parameters with empirical parameters indicated by the remaining systematic image errors. This avoids strong correlations. The parameter set in BLUH was later reduced to the important parameters (Jacobsen 2007) and extended to include parameters such as the corner parameters (5), which are often required by not completely flat digital sensors – formally, this was not required for analogue cameras with a pressure plate.

For fused camera-system data, physically based parameters are required that take the camera system's metric into account. The basic information required are shifts of the sub-images in x and y relative to a reference sub-images. Additionally, rotations and a scaling factor, or a perspective correction, of the image part covered by a sub-image, may be required.

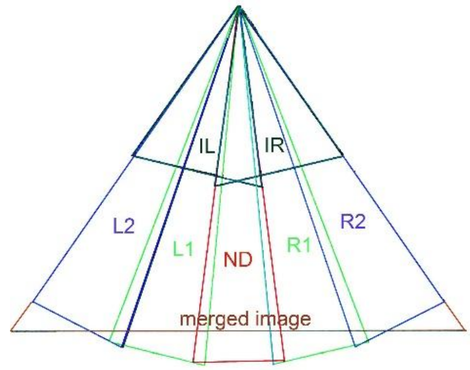

Figure 4: Combination of PAS Pana fields of view

The additional systematic image errors of the PAS Pana are limited to the sub-images by the x-coordinates of the fused images of +/-15.77 mm and +/-49.315 mm (Figures 1 and 4). This respects the reduction of the focal length from 146 mm to 132 mm to compensate for the image enlargement due to the projection.

Additional parameters of Brown-Conradi (Australis)

$x = x_{meas} - xp \qquad y = y_{meas} - yp \qquad$ (1) inner orientation
x, y = image coordinates
xp, yp = principal point
$r^2 = x^2 + y^2$
$dr = K1 * r^3 + K2 * r^5 + K3 * r7 \qquad$ (2) radial symmetric

K1, K2, K3 radial symmetric distortion parameters

$x_{corr} = x_{meas} - xp - x*dr/r + P1*(r^2+2*x^2)+2*P2*x*y + B1 * x + B2*y$

$y_{corr} = y_{meas} .yp + y*dr/r + P2*(r^2 + 2*y^2) + 2*P1*x*y \qquad (3)$

P1, P2 decentering distortion parameters
B1, B2 affinity and angular affinity (non-orthogonal)
(2) + (3) = Brown-Conradi (Australis) self-calibration parameters (User Manual for Australis, 2007)

Basic additional parameters of BLUH (4)
x, y = image coordinates normalized to maximal radial distance 162.6mm (scale factor: 162.6 / maximal radial distance)
$r^2 = x^2 + y^2 \qquad b = \arctan(y/x)$
1. $x' = x - y \bullet P1 \qquad y' = y - x \bullet P1$
2. $x' = x - x \bullet P2 \qquad y' = y + y \bullet P2$
3. $x' = x - x * \cos 2b \bullet P3 \qquad y' = y - y \bullet \cos 2b \bullet P3$

4. $x' = x - x \bullet \sin 2b \bullet P4$ $\quad y' = y - y \bullet \sin 2b \bullet P4$
5. $x' = x - x \bullet \cos b \bullet P5$ $\quad y' = y - y \bullet \cos b \bullet P5$
6. $x' = x - x \bullet \sin b \bullet P6$ $\quad y' = y - y \bullet \sin b \bullet P6$
7. $x' = x + y \bullet r \bullet \cos b \bullet P7$ $\quad y' = y - x \bullet r \bullet \cos b \bullet P7$
8. $x' = x + y \bullet r \bullet \sin b \bullet P8$ $\quad y' = y - x \bullet r \bullet \sin b \bullet P8$
9. $x' = x - x \bullet (r^2 - 16384) \bullet P9$ $\quad y' = y - y \bullet (r^2 - 16384) \bullet P9$
10. $x' = x - x \bullet \sin(r \bullet 0.049087) \bullet P10$ $\quad y' = y - y \bullet \sin(r \bullet 0.049087) \bullet P10$
11. $x' = x - x \bullet \sin(r \bullet 0.098174) \bullet P11$ $\quad y' = y - y * \sin(r \bullet 0.098174) \bullet P11$
12. $x' = x - x \bullet \sin 4b \bullet P12$ $\quad y' = y - y \bullet \sin 4b \bullet P12$

Corner Parameters of BLUH (5)

½ image format

81. for $x>0$, $y<0$: $x' = x - x^2 * y^2 * \mathrm{abs}(x*y) * P81$ tangential
“ $y' = y + x^2 * y^2 * \mathrm{abs}(x*y) * P81$

82 – 84 for other image quarters

85. for $x>0$, $y<0$: $x' = x + x^2 * y^2 * P85$ radial
“ $y' = y + x^2 * y^2 * P85$

86 – 88 for other image quarters

1/6 image corners Δx and Δy for image corners

90. for $x>0.67*xmax$, $y<-0.67*ymax$:
$x' = x - \Delta x^2 * \Delta y^2 * \mathrm{abs}(\Delta x * \Delta y) * P90$
radial “ $y' = y - \Delta x^2 * \Delta y^2 * \mathrm{abs}(\Delta x * \Delta y) * P90$

91 – 93 for the other quarters

94. for $x>0.67*xmax$, $y<-0.67*ymax$:
$x' = x - \Delta x * \Delta y * (\Delta x^2 + \Delta y^2) * P90$
tangential “ $y' = y + \Delta x * \Delta y * (\Delta x^2 + \Delta y^2) * P90$

95 – 97 for other quarters

Additional parameters in BLUH for PAS Pana, limited to the sub-areas of the single images (6) [mm]

a) Shift in x
b) Shift in y
c) Rotation around the projection centre of the sub-images, respecting the projection
d) Related to start of sub-image left as curvature with function of x by (ΔX from left) $* y^2$
e) Related to start of sub-image right as curvature with function of x by ($-\Delta X$ from right) $* y^2$
f) Affinity
g) Angular affinity
h) for the nadir sub-image

For the nadir sub-image, only the rotation c) and the curvature d) and e) are used.

In addition to the basic parameters (4) and additional parameters for special purposes, a total of up to 30 special additional parameters are used for the PAS Pana. The additional parameters are tested for significance, correlation and total correlation. The total correlation is a value that describes how the effect of an additional parameter is replaceable by the sum of all other additional parameters. Based on significance, large correlation and total correlation, the program BLUH used excludes unnessary additional parameters from the block adjustment by default. When fitting the basic BLUH parameters (4), plus corner effects (5), plus the special PAS Pana parameters (6), only 3 of 59 parameters were not accepted by BLUH and this was caused due to low values (Table 1). In Table 1 only the parameters 176, 177 and 181 (“000” behind the parameters are for possible different camera sets) are excluded due to small values of the Student test. The Student test is the ratio of the value of a parameter divided by its own standard deviation.

ADDITIONAL PARAMETERS

1	1000	2000	3000	4000	5000	6000	7000	8000	9000	10000	11000	12000
2	14000	15000	81000	82000	83000	84000	85000	86000	87000	88000	160000	161000
3	162000	163000	164000	165000	166000	167000	168000	169000	170000	171000	172000	173000
4	174000	175000	176000	177000	178000	179000	180000	181000	182000	183000	184000	185000
5	186000	187000	188000	189000	190000							

STUDENT TEST

1	172.68	33.50	133.85	92.32	76.35	1.15	240.96	214.89	197.87	16.38	1.14	126.24
	+++	+++	+++	+++	+++		+++	+++	+++	+++		+++
2	11.27	5.95	27.81	4.69	16.67	59.29	50.27	15.83	6.31	57.47	7.46	3.76
	+++	+++	+++	+++	+++	+++	+++	+++	+++	+++	+++	+++
3	66.15	50.98	88.18	96.16	117.81	51.84	37.78	70.09	52.92	105.32	22.64	1.40
	+++	+++	+++	+++	+++	+++	+++	+++	+++	+++	+++	
4	5.64	8.81	0.08	0.30	5.31	5.82	13.52	1.70	2.55	7.54	12.77	0.67
	+++	+++			+++	+++	+++		+	+++	+++	
5	17.48	34.73	47.33	90.99	20.01							
	+++	+++	+++	+++	+++							

Table 1: Student test of a block adjustment of the basic BLUH parameters, plus corner effects, plus the special PAS Pana parameters

In Table 1, the “***” under the Student-test value indicates the significance level of the parameter, “*” is significant on 95% level, “**” is significant on the 99% level and “***” is significant on the 99.9% level. The high significance also is due to the 1.26 million image coordinates used.

Special additional parameters for DMC-1, limited to the sub-area of the single cameras (7)

a) for the whole merged area:

$x' = x + (0.9 * |x| + 1.11*|y|)*x$
$y' = y + (1.11*|y| + 0.9*|x|) * y$

for each of the image sub-areas:

b) $x' = x + x^2 +/- 32. * x$
$y' = y$
c) $x' = x + x * y$
$y' = y$
d) $x' = x$
$y' = y + x * y$
e) same r^3 for images + perspective transformation

Special additional parameters for UltraCam Eagle (8)

For all image sub-areas without centre part 3 (Figure 3):

a) Scale
b) Shift x
c) Shift y
d) Perspective transformation
e) Rotation of sub-images
f) $x' = \Delta x * \Delta y$ coordinates in sub-images

3. Experiences

The development of the additional parameters is based on the analysis of bundle block adjustments. Remaining systematic image errors after self-calibration with additional parameters can be analysed using residuals at the image coordinates after bundle block adjustment. This method has the advantage, that it avoids strong correlations between the existing and newly introduced additional parameters.

3.1 Leaf P80 single camera

In 2014 a Leaf P80 was calibrated using a photo flight over a three-dimensional test field in Ica, Peru with crossing flight lines, 60% side lap and 60% forward overlap at two flight elevations with 8cm Ground Sampling Distance (GSD) and with 20cm GSD. The calibration of this single camera with 5.2 µm pixel size is included to show the requirement of corner parameters.

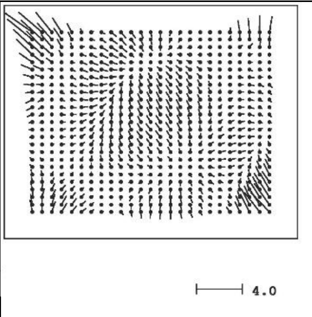	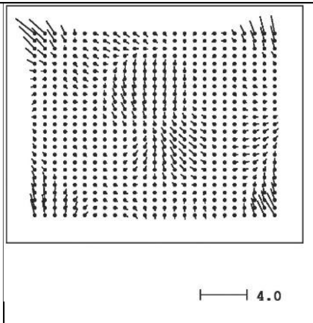
Based on Brown parameters Sigma0= 2.08 µm remaining: Sx=0.42 Sy=0.48 max 3.55	Based on BLUH parameters Sigma0= 2.05 µm remaining: SX=0.30 Sy=0.42 max=2.77

Figure 5: remaining systematic image errors [µm] Ica test block

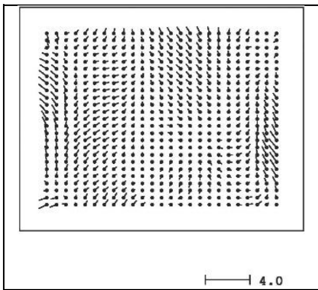	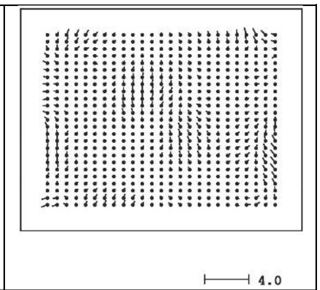
With Brown parameters Sigma0=2.05µm remaining: Sx=0.30 SY=0.37 max=1.91	With BLUH parameters Sigma0=2.05µm remaining: Sx=0.21 Sy=0.30 max=1.34

Figure 6: remaining systematic image errors, adjustment with corner parameters 81 – 88 [µm] Ica test block

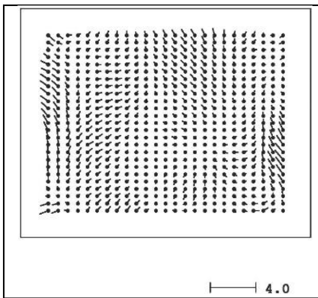	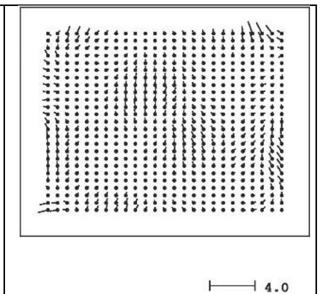
With Brown parameters Sigma0=2.04µm remaining: Sx=0.30 SY=0.35 max=1.89	With BLUH parameters Sigma0=2.04µm remaining: Sx=0.21 Sy=0.28 max=1.42

Figure 7: Remaining systematic image errors, adjustment with corner parameters 81 – 88 + 90 - 97 [µm] Ica test block

The bundle block adjustment with 421 images and a total of 127000 image points, with an average of 7 images per object point, was computed using the BLUH (4) and the Brown-Conradi parameters (1 up to 3) (Fig. 5) extended by more additional parameters. The remaining systematic image errors show significant corner deformations, which are slightly larger when computed with the Brown-Conradi parameters than with the basic BLUH parameters. For this reason, the block adjustments were repeated with the corner parameters 81 up to 88 (5). This reduced the remaining systematic image errors of the computed image grid in the image corners (Figure 6) from a maximum of 3.55 µm, and 2.77 µm, respectively, to 1.91 µm for the combination with the Brown-Conradi parameters and to 1.34µm for the combination with the BLUH parameters. Based on experience with some other cameras, corner parameters 90 – 97 were also included (Figure 7). Although this further reduced the remaining systematic image errors, the improvement was not really necessary. Finally, it became clear that the corner parameters should be taken into account. In the block adjustment with corner parameters 81 up to 88, all additional parameters were significant. In the adjustments with in addition the corner parameters 90 to 97, 6 of the 29, and 34 parameters, respectively, were not significant.

3.2 DMC-1

The DMC-1 is based on four slightly convergent viewing sub-cameras (Figure 2). Figure 2 is not correct in detail because the projection centres of the sub-cameras are offset (Figure 8).

$$DX = \frac{\Delta h \bullet DX0}{hg} \qquad DY = \frac{\Delta h \bullet DY0}{hg} \qquad (9)$$

Geometric influence of the differences between the projection centers to ground coordinates

hg = flying height above ground

Δh = object height above reference plane

The offset of the projection centers is 11.7 cm (DX0) in the direction of flight and 21.5 cm (DY0) across flight direction. If the object points lie in the same plane, the height difference Δh is 0.0, meaning the offset of the projection centers has no influence on the ground position. This is not the case for difference in height Δh.

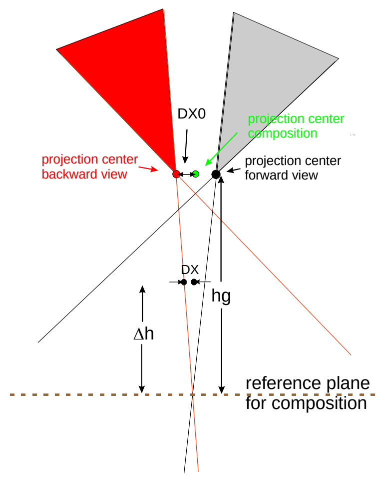

Figure 8: Geometric influence of the differences between projection centers to object points located in different altitude

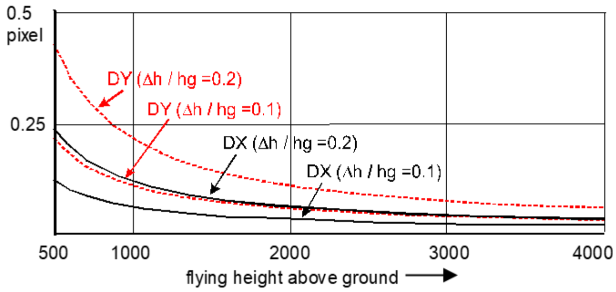

Figure 10: Influence of differences between projection centers to image for relative height differences in object space of Δh/hg = 0.1 and 0.2

The projection center offset problem exists in almost all camera systems, but in most cases it is smaller than with the DMC-1. If the offset is not respected for image fusion, the largest part is eliminated by the fusion. As shown in Figure 10, it is larger at lower flight altitudes and smaller for smaller height differences within the covered image area. This obviously slightly affects the image geometry, but depends on the digital elevation model, so most of it is random for the image block.

The DMC-1`s image fusion is based on tie points in the overlapping areas by bundle adjustment of the 4 sub-images. The convergent arrangement of the sub-cameras enables a three-dimensional bundle adjustment of any combination of the four sub-cameras. For imaged water surfaces, the orientation of the previous sub-image combination is used. It has been shown that the focal length should be used as unknown, due to thermal changes of the camera system. A bundle block adjustment of the DMC-1 fused images from a photo flight typically results in a sigma0 in the range of 1µm for the 12 µm pixel size. The additional parameters (7) were generated according to the camera geometry. Only the parameters (7 a and 7 e) that can compensate for an incorrectly used flying elevation for the image fusion and the radial symmetric distortion for the sub-images were significant, but had an influence for the fused images only in the range of 0.1µm (Doerstel et al.2002).

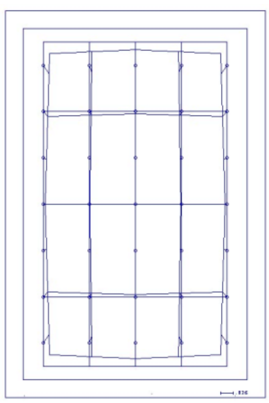

Figure 11: Effect of wrong flying height for the image fusion

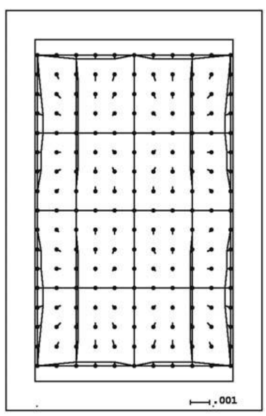

Figure 12: Same r³ for all sub-images + perspective transformation

3.3 Vexcel UltraCAM-D

As shown in Figure 3, the Vexcel UltraCam is based on nine sub-images from four sub-cameras. Originally, the sub-images were fused by stitching the nine neighboured sub-images together. This resulted in non-negligible systematic errors that had to be determined and respected with the additional parameters (8 a - d). For this reason, Vexcel modified the fusion of the sub-images by transforming the panchromatic high-resolution sub-images to the homogenous green image (Leberl et al. 2002). Nevertheless, minor remaining systematic image errors remained (Figure 13). More importantly, the additional parameters (8 e and f), slightly improved the results of the bundle block adjustment (Jacobsen 2007).

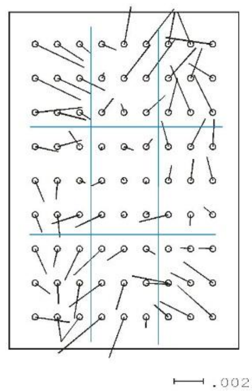

Figure 13: remaining systematic image errors of an UltraCam-D (Baz et al, 2007)

More important are the general additional parameters for the fused images, which can improve the accuracy of the bundle block adjustment.

3.4 **PhaseOne PAS Pana**

The PhaseOne PAS Pana is one of the latest camera systems with fife RGB sub-cameras and two NIR sub-cameras (Figures 1 and 4). The PAS Pana sub-images were fused into joint images by transforming the RGB sub-images into the joint NIR images (Jacobsen et al. 2025).

The geometry of the fused PAS Pana images was tested using the Denver photo flight taken from approximately 6000m above ground, resulting in a ground resolution of 17cm for the fused images (Figure 4). The north-south flight strips have 40 % side overlap and 75 % end overlap. Two crossing flight lines cover 44% of the total area. There are 718 images with 193818 ground points and 1.2 million image points and in the average 6.2 images per object point, allowing for detailed analysis. For image fusion, the image geometry was modified by laboratory calibration using the Brown-Conradi parameters. The bundle block adjustment without self-calibration resulted in a sigma0 of 1.13 µm, corresponding to the standard deviation of the image coordinates, which is a satisfactory result for the pixel size of 3.76 µm.

By failure, for the image fusion not the correct calibration data and rotation of the calibration data for the sub-cameras were used. This led to specific problems for the image geometry, which should be solved with the newly introduced additional parameters

(6 d and 6 e) (curvature of the sub-images). The geometric problems became obvious when computing the remaining systematic image errors based on the bundle block adjustment without self-calibration (Figure 14). This shows significant systematic effects caused by improper handling of the calibration data. Nevertheless, the systematic errors are small with root mean square image coordinate errors in x of 0.27 µm and in y of 0.47 µm, with a maximal value of 1.8 µm.

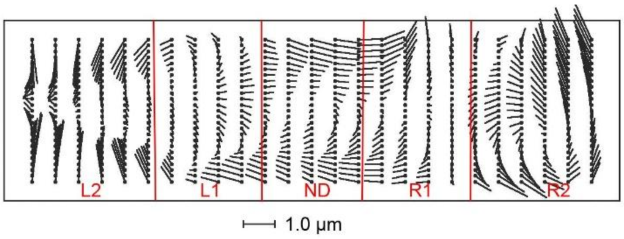

Figure 14: Remaining systematic image errors of PAS Pana fused images using incorrect calibration data, determined by adjustment without self-calibration with the area of the sub-images in red

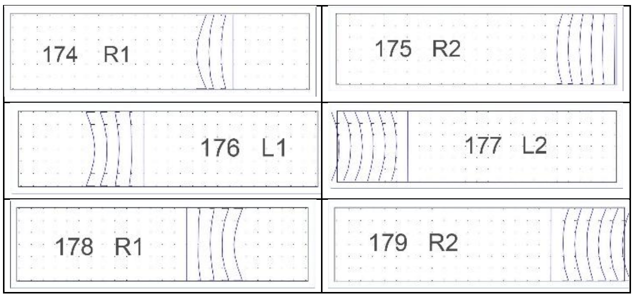

Figure 15: Influence of special PAS Pana additional parameters separated for the sub-areas of the sub-cameras

The remaining systematic image errors are small but can be improved by special additional parameters, as shown in Figure 15, using a function of $dx = y^2 * x$, where x is the coordinate within the sub-area, counting from left and additionally from right. A higher number of additional parameters must be used; this has to be tested for significance and correlation. If the new additional parameters are based on the analysis of remaining systematic image errors, they are automatically not strongly correlated. Only 4 of 56 additional parameters are not significant and can be eliminated.

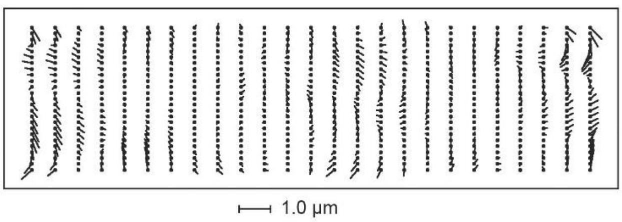

Figure 16: Remaining systematic image errors based on the BLUH parameters 1-15, corner parameters 81-86 and the special PAS Pana parameters 160 – 194

Figure 16 shows the remaining systematic image errors based on the basic BLUH parameters, corner parameters, and the special PAS Pana parameters. The remaining systematic errors are very small, with root mean square image coordinate errors in x of 0.12 µm and in y of 0.18 µm (0.15 pixels), with a maximal value of 1.0 µm. The sigma0 is reduced by 16 % from 1.13 µm to 0.95 µm. A further reduction of the systematic image errors is nearly impossible.

6. CONCLUSION

Systematic errors in single camera images, the difference between the perspective image geometry and the real camera geometry, can be significantly reduced by using standard sets of additional parameters in the block adjustment. Although the Brown-Conradi parameters have some limitations, the major part of the systematic parameters can be eliminated. Important parameters are corner parameters, which cannot be neglected for several cameras used.

Due to the limited size of available CMOS sensors, camera systems are required to cover larger areas. Single cameras can have a thermal control that improves the camera geometry, but this is not possible with camera systems. Camera systems can introduce additional geometric problems depending on the geometric arrangement of the sub-cameras and the method of image fusion. This arrangement can vary considerably and requires special sets of additional parameters for each camera system.

As the PAS Pana data set from the Denver test flight demonstrates, not only can standard systematic errors be determined and respected, but errors in the handling the calibration data can also be compensated. By analyzing the remaining systematic image errors, the necessary additional parameters can be constructed to eliminate the geometric problems. With proper image fusion and sets of additional parameters, with the fused images the same accuracy can be achieved as with single images.

References

Brown, D., 1971. Close-range camera calibration. Photogrammetric Engineering, 37(8), 855–866.

Conrady, A. E., 1919. "Decentred Lens-Systems". Monthly Notices of the Royal Astronomical Society. **79** (5): 384–390.

Doerstel, C., Zeitler, W., Jacobsen, K., 2002. Geometric Calibration of the DMC: Method and Results, IntArchPhRS (34) Part 1 Com I, pp 324 – 333

Ebner, H., 1976. Self Calibrating Block Adjustment. IntArchPhRS Vol. 21, Part 3, Commission III, ISP Congress, Helsinki.

Grün, A., 1978. Experiences with Self-Calibrating Bundle Adjustment. Presented Paper, *AS Convention, Washington D.C.*, Febr./March.

Gruen, A. and Beyer, H., 2001. System Calibration Through Self-Calibration. In: Gruen, A. and Huang, T. S. (editors), *Calibration and Orientation of Cameras in Computer Vision.* Springer-Verlag, Berlin Heidelberg, pp. 172-180.

This contribution has been peer-reviewed.
https://doi.org/10.5194/isprs-archives-XLVIII-1-W4-2025-49-2025

Gruber, M.,Ladstädter, R. 2006. Geometric issues of the Digital Large Format Aerial Camera, International Calibration and Orientation Workshop, EuroCOW 2006, Castelldefels, on CD

Jacobsen, K., 2007a. Geometric Handling of Large Size Digital Airborne Frame Camera Images, Optical 3D Measurement Techniques VIII, Zürich 2007, pp 164 -171

Jacobsen, K., 2007b. Geometry of Digital Frame Cameras, ASPRS annual conference, Tampa 2007

Jacobsen, K., 1980. Vorschläge zur Konzeption und zur Bearbeitung von Bündelblockausgleichungen, Phd thesis, Wissenschaftliche Arbeiten der Fachrichtung Vermessungswesen der Universität Hannover

Jacobsen, K., Cramer, M., Ladstaedter, R., Ressl, C., Spreckels, V., 2010. DGPF project: Evaluation of digital photogrammetric camera systems - geometric performance. PFG 2010 (2), pp 85 – 98

Jacobsen, K., Ladstaedter, R., Bosch, R., 2025. Geometric Accuracy of PhaseOne PAS Pana, Topographic Mapping from Space, Istanbul, ISPRS Archives 2025

Leberl, F., Perko, M., Gruber, M., Ponticelli, M., 2002. Novel Concepts for Aerial Digital cameras, ISPRS Com I, Denver 2002, ISPRS Archive Vol. 34 Part 1

Schut, G.H. 1974. On correction terms for systematic errors in bundle adjustment

Tang. L., Dörstel, C., Jacobsen, K., Heipke, C., Hinz, A, 2000. Geometric Accuracy Potential of the Digital Modular Camera, ISPRS Congress, IntArchPhRS. Vol XXXIII, Vol B4/3 pp 1051 – 1057

User Manual for Australis 2007 – Photometric Photogrammetry Software, photometrix.com.au, Access May 2025